

BIOENGINEERING LABORATORY 210

TERM PROJECT:
*THE EFFECTS OF OXYGEN DURING GAMMA
RADIATION STERILIZATION OF ULTRA-HIGH
MOLECULAR WEIGHT POLYETHYLENE*

Group R2
Siddharth Fernandes
Summit Gupta
Richard Kiok
Andrew James

Submitted April 30, 1997

TABLE OF CONTENTS

SECTION	PAGE
Abstract	2
Acknowledgments	3
Background	
Introduction	5
Biological Uses of UHMWPE	5
Gamma Radiation Sterilization	6
Oxidative Degradation of UHMWPE	6
Apparatus and Materials	9
Procedure	
Differential Scanning Calorimetry	10
Three-Point Bending	10
Hardness Testing	12
Results	14
Error Analysis	18
Discussion	
Significant Findings	22
Quantitative Error Analysis	22
Limitations of the Findings and Possible Experimental Alterations	24
Theoretical Explanation of Results	26
Appendix A: PE Terminology	
Amorphous vs. Crystalline PE	29
Linear vs. Branched PE	29
Appendix B: Data	
Compression and Hardness Testing	31
Three-Point Bending	31
Differential Scanning Calorimetry	33
References	35

ABSTRACT

The experimental goal was to determine the effects of oxygen on ultra-high molecular-weight polyethylene (UHMWPE) samples after gamma irradiation in two different environments—one inert and the other oxygenated. The material properties of two UHMWPE knee implants, one gamma irradiated in argon and the other gamma irradiated in air, were examined. Gamma radiation tends to enhance the oxidation of UHMWPE by forming free radicals via chain scission. Research has shown that oxidation is directly correlated with increased crystallinity. Researchers believe that this increase in crystallinity is responsible for the mechanical failure of the polyethylene *in vivo*.

Three types of mechanical tests were performed: differential scanning calorimetry (DSC), three-point bending, and hardness testing. The DSC testing provided heat of fusion and percent crystallinity data. DSC testing was performed twice, once at Day 1 and again at Day 15, in order to determine if appreciable oxidation could occur in a relatively short period of time. It was found that the percent crystallinities of the argon sample at Day 1 and Day 15 were the same within the 95% confidence limit (Day1: 82.6% \pm 1.02%, Day15: 82.1 \pm 1.35%). The same was true of the air sample (Day1: 80.7% \pm 1.81%, Day15: 80.2 \pm 1.82%). Comparing air and argon, it was found that they had similar crystallinities (on Day1 and Day 15) and heat of fusion values (argon: 128 J/g \pm 2.03%, air: 132 J/g \pm 3.05%), as well. From the hardness testing, the Brinell hardness numbers for the two sets of samples were statistically the same (argon: 48.4 MPa \pm 2.27%, air: 49.7 MPa \pm 3.38%). The three-point bending test provided the Young's modulus values (E) and the yield strength of both samples. It was found that the Young's modulus of the air samples was statistically different from that of the argon samples (argon: 1.19 GPa \pm 12.4%, air: 2.03 GPa \pm .841%). The same holds true for the yield strength of the two sets of samples (argon: 45.2 MPa \pm 14.4%, air: 69.8 MPa \pm 12.6%).

ACKNOWLEDGMENTS

We would like to thank:

- Professor William R. Graham and Dr. Fred Allen for their assistance in shaping the nature, focus, and goals of our project;
- The staff of the LRSM labs, notably Dr. Alex Radin and Scott Norin, for their aid in performing the physical tests on our samples; and
- The members of Group W4 (Kevin Justice, Joanna Law, Seungtaek Lee, and Kathryn Rothman) for sharing their data, thoughts, and hypotheses in order to make our projects complementary and cooperative efforts.

BACKGROUND

INTRODUCTION

Total joint replacement is frequent and costly. An estimated 120,000 total hip replacements and 120,000 total knee replacements are performed in the United States annually. The total hospital and physician cost for each procedure is generally between \$25,000 and \$30,000 (Ward & MacWilliam, 1995). And in Ontario, Canada, (where health care is governmentally subsidized) 6,200 hip and 5,000 knee replacements were performed in 1991. The costs of surgery are covered by hospital budgets including the prostheses, cost of the operation, acute follow-up care and in-hospital rehabilitation. However, joint replacement is considered an elective procedure for most cases. Therefore, some hospitals cap the number of prostheses ordered and limit operating time (Williams, J. I. et al., 1991). Typically, the life expectancy of a replaced joint is 15 years (Candor Technologies, 1996). Because of the high cost of the procedures and the potential waiting times, increasing the life expectancy of the artificial joint prostheses would be beneficial to both hospitals and patients.

In the past, artificial knee replacements lasted only a few years before failing due to fracturing or loosening of femoral or tibial components. Improvements in knee design has resulted with polyethylene wear leading to failure of the insert as the limiting factor in longevity of a total knee system. One approach developed in the lab was to make the insert easily removable so that a minor surgery could be used to replace it. While this approach has provided new life to an artificial knee joint, wear debris has been shown to cause bone loss (Orthopedics Research Lab, University of Arizona, 1995). Thus, it has become necessary to increase the longevity of the ultra high molecular weight polyethylene (UHMWPE) articulating surface.

BIOLOGICAL USES OF UHMWPE

Ultra high molecular weight polyethylene is a linear polyethylene (Appendix A: PE Terminology) that has an extremely high molecular weight, approximately 4×10^6 g/mol, which is an order of magnitude greater than that of the high density polyethylene (HDPE). The increased molecular weight gives UHMWPE extraordinary characteristics that become important in the biological system:

1. An extremely high impact resistance.
2. Outstanding resistance to wear and abrasion, leading to longer life expectancy of the prosthesis.
3. A very low coefficient of friction, making it a natural choice as an articulating surface.
4. Very good chemical resistance and excellent biocompatibility.

5. Excellent low-temperature properties suitable for ambient body conditions.

However, it has a relatively low melting temperature, so its chemical and mechanical properties diminish rapidly with increasing temperature (Callister, 1997). These properties make UHMWPE an excellent articulating surface in artificial joint replacements. It is used in the acetabular cup of the artificial hip as well as a replacement for cartilage in the artificial knee prosthesis.

GAMMA RADIATION STERILIZATION

Gamma radiation has been shown to be both cost effective and very effective as a sterilization procedure. It is a penetrating sterilant, and therefore, no area of the sample being sterilized is left with uncertain sterility. "Penetrating" has two implications: 1) it penetrates all surfaces and cavities of the sample, and 2) it penetrates protective spores formed by bacteria, unlike surface sterilants such as ethylene oxide (EtO) and autoclave, in order to kill them (ZEUS, Inc.).

Gamma rays high energy electromagnetic waves that are emitted from radioactive materials such as Cobalt 60 and Cesium 137. Cobalt 60 has become the industry standard because:

1. Its reliability is unmatched, stemming from the extreme penetrating nature of gamma radiation and the ease of controlling the single sterilization process variable - TIME.
2. There are no chemical residues on products after sterilization.
3. The effectiveness of the sterilization process is not affected by the use of hermetically sealed packages, or by products containing sealed cavities (Isomedix).

The sample being sterilized is placed near the emitting source until the required amount is absorbed. The radiation effectively kills any microorganism that may be present on or within the sample. The sample absorbs no radiation during the sterilization procedure. Thus, it can be used immediately after being sterilized.

OXIDATIVE DEGRADATION OF UHMWPE

Gamma radiation of UHMWPE results in the formation of free radicals through the chain scission of polymer chains. These free radicals react with available oxygen in the environment (whether *in vitro* or *in vivo*) and become oxidized. Oxidation results in shorter UHMWPE molecules with keto-carbonyl groups. In turn, this leads to a polymer with a lower molecular weight and resembles high density polyethylene, HDPE (Naidu et al., 1996 and Sutula et al., 1995).

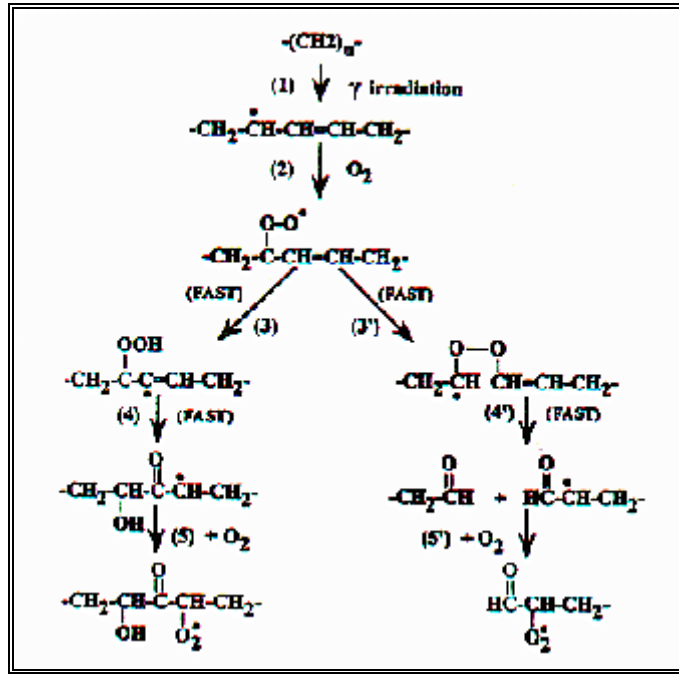


Figure 1: Schematic diagram of the free-radical oxidation mechanism (Naidu et al., 1996).

A review of the literature shows that oxidation of UHMWPE continues for long periods of time after gamma radiation (Li et al., 1994).

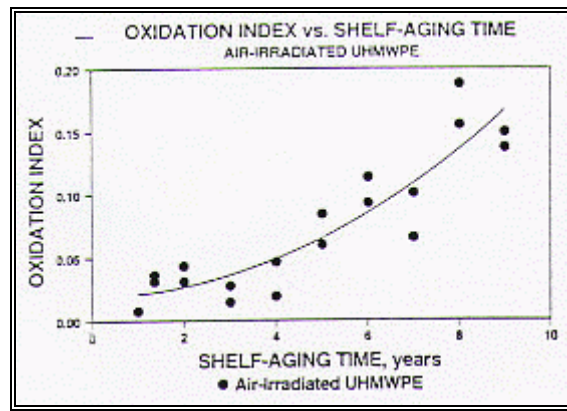
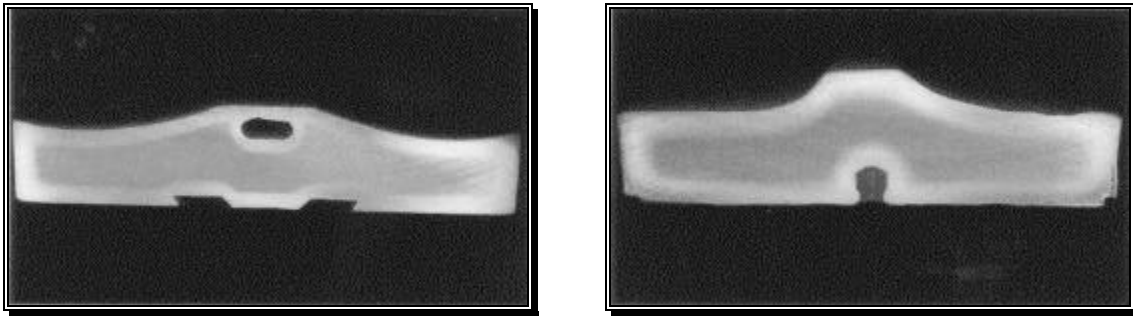


Figure 2: Oxidation-Aging Time Correlation (Naidu et al., 1996).

Similarly, it has been suggested that argon and other gamma inert gases (such as nitrogen) cannot eliminate oxidation due to the presence of dissolved oxygen within the polyethylene (Wright Medical Technology, Inc., 1995). The high energy gamma rays tend to accelerate the oxidation. Furthermore, Ries et al. have shown that sterilization in inert gas does not prevent free radicals from causing oxidation for this reason. In fact, the majority of oxidation occurs during post-radiation aging and not during the sterilization process. The initial inert environment in which the polyethylene sample was sterilized dissipates as a function of time. Oxygen continuously permeates the package after

sterilization. Therefore, the UHMWPE is exposed to oxygen during the critical aging period. And, since oxygen is dissolved in polyethylene by means of its manufacturing, it follows that gamma radiation is not necessary for the oxidation mechanism. Finally, oxidation may continue *in vivo*, due to oxidants within the body (Wright Medical Technology, Inc., 1995). “Air tight” packages are not necessarily “diffusion tight.” Irradiation in an inert atmosphere can eliminate short-term oxidation but cannot prevent oxidation in the long term (Sun et al., 1996).

Oxidation is directly proportional to the amount of oxygen available. Thus, it is logical that the surface of polyethylene implants will have higher degrees of oxidation than inner surfaces. The degree of oxidation can be determined by examining the differences in color (darkness) between the oxidized “white bands” and other parts of the implant. Diffusion of oxygen has been documented as the limiting factor in oxidative degradation of polyethylene (Naidu et al., 1996).



Figures 3, 4: Cross-sections of oxidized UHMWPE knee implants showing oxidative “white bands” and an oxidation gradient.

Free radicals tend to react differently in inert and oxygenated environments. As stated, free radicals in the presence of oxygen tend to oxidize and break the C-C or C-H bonds of the polymer chain. However, there are other possible free radical reactions. The two carbon radicals may react with one another to form crosslinks (C-C bonds between different polymer chains). This is the minority reaction in oxygenated atmospheres and the majority reaction in inert atmospheres (Sun et al., 1996).

APPARATUS AND MATERIALS

1. Differential Scanning Calorimetry
 - Perkin Elmer DSC7
 - Perkin Elmer Autobalance
2. Density Gradient Column
 - Ethyl Alcohol: Density = 0.7873 g/cm^3 .
 - Water: Density = 1.00 g/cm^3 (Lide, 1994).
3. Three-Point Bending
 - Instron Testing Machine Model 1331
 - Lebow Load Cell Model 3170-208
 - Cervo Hydraulic System
4. Hardness Testing
5. Polyethylene Samples
 - Air-irradiated UHMWPE knee implant.
 - Argon-irradiated UHMWPE knee implant.



Figure 5: UHMWPE knee implant *in vivo*.

PROCEDURES

DIFFERENTIAL SCANNING CALORIMETRY

Small pieces (approximately 10 mg) of the oxygen sterilized (n = 4) and argon sterilized (n = 7) samples were cut from the prosthesis in order to be placed in the pans of the differential scanning calorimeter (DSC). Two empty pans and lids were weighed and the difference was autotared in the Perkin-Elmer Autobalance for each sample. Both pans were hermetically sealed, one with the sample and the other one empty (to be used as a reference). The pans were placed back in the Autobalance and the difference was recorded as the weight of the sample. Inserting both pans into the DSC7 a test was run to determine the melting temperature of the polyethylene sample from a range of temperature of 50 °C to 175 °C at a rate of 10 °C/min. The plot of temperature vs. heat flow was printed to be analyzed later. This test was performed twice times; once on the first week and once on the third week.

Indium was used as a calibration standard. The indium sample was prepared and tested in the same manner as the polyethylene samples. The plot of temperature vs. heat flow was taken to represent a sample of 100% crystallinity.

In order to analyze the temperature-heat flow graphs, each set of data was rescaled to create a graph with an area of 2,025 mW-°C (usually 45 °C x 45 mW). The graphs were physically cut out and weighed. The mass of the curve was then multiplied by a calibration factor (converting mg to square cm) to determine the area of each curve. The crystalline and amorphous portions were separated and weighed independently. Percent crystallinity was then calculated using the equation:

$$\boxed{\% \text{ Crystallinity} = \frac{\text{Crystalline Area}}{\text{Total Area}}}$$
 Eq. 1

THREE-POINT BENDING

In order to reduce the uncertainty imposed by the irregular geometry of the samples, they were cut into rectangular solid pieces. Measurements of all dimensions were taken. Notches were created in the polyethylene samples using a hydraulic press that pushed the sample against a knife blade at a 90° (right) angle. They were created in order to concentrate stress at a particular region of the sample. By measuring the depth of the notch, the affected area (for use in the calculation of stress) could be determined.

The Instron Testing Machine Model 1331, Lebow Load Cell Model 3170-208, and the Cervo Hydraulic System were arranged to determine the Young's Modulus (E) of the two UHMWPE samples during three point bending (oxygen: n = 2, and argon: n = 2). The Instron

was carefully lowered so it was extremely close to the samples without touching them. The test began by applying a measured load from the crosshead of the Instron to the middle of the sample. The applied load was plotted with the displacement sample, until the yield point had been exceeded. The test was performed twice on each sample; once concentrating stress on the notched region and once on a region that remained unnotched. To translate the force vs. displacement curves to stress vs. strain curves the equations

$$\mathbf{s} = \frac{LP}{\left(\frac{8}{12} wx^2\right)} \quad \text{Eq. 2}$$

$$\mathbf{e} = \frac{12 xg}{L^2} \quad \text{Eq. 3}$$

were used where σ and ϵ are the stresses and strains corresponding to the load, P, and displacement, γ , respectively. W is the width of the sample, x is the difference between the height of the sample and the notch size, and L is the length of the sample.

Linear regression was performed on each stress vs. strain graph to find the slope of the best fit line through the linear portion of the graph, which was at the beginning of the graphs. The linear portion of the graph corresponds to the polyethylene sample undergoing elastic deformation. The slope of the regression line represents the best value of the Young's modulus for the respective polyethylene sample.

The stress vs. strain graphs were also used to find the yield strength of the samples. For each sample the yield strength that corresponded to a 0.2% offset in the strain of the sample was found. On each of these graphs the intersection of the "0.2% offset" line, $\mathbf{s} = E(\mathbf{e} - 0.002)$, with the stress vs. strain curve was found. The stress corresponding to each of these intersections corresponded to the yield point of the sample.

To find the intersection of the "0.2% offset line" with the stress vs. strain curve, best fit line through the region of the stress vs. strain curve which was speculated to contain the yield point of the polyethylene sample, was found. To find this best fit line, a pair of stress/strain data points in the region of the stress vs. strain curve were taken. The best fit line through the region of the stress vs. strain curve was found to be the line containing the pair of stress/strain data points. The difference of the stresses corresponding to these points divided by the difference in the strains corresponding to these points gave the slope of the best fit line. Subtracting the stress corresponding to one of the data points with the product of the slope and the strain of the same data point gave the y-intercept of the line. Simple algebra was used to find the intersection of this best fit line with the "0.2% offset" line and

was taken to be the same intersection of the stress vs. strain curve with the “0.2% offset” line.

HARDNESS TESTING

Two carbide plates, chosen for their superior hardness, were placed on either end of the Instron machine. Following this the sample was mounted onto the first piece of carbide. A stainless steel ball was then mounted onto the sample. Petroleum jelly was used to hold it into place as the second carbide piece was pushed in by the Instron. Following this the steel ball would compress the surface making an indentation. Force vs. displacement graphs were used find the Brinell hardness numbers of the polyethylene samples. For each graph (corresponding to one polyethylene sample), load that corresponded to the vertical displacement of 0.000625m, was found. To calculate the diameter of the hole corresponding that vertical displacement, the formula

$$d = 2 \cdot \left[\left(\frac{D}{2} \right)^2 - \left(\frac{D}{2} - s \right)^2 \right]^2 \quad \text{Eq. 4}$$

was used where d is the diameter of the hole, D is the diameter of the ball, and s is the vertical displacement. The diameter of the hole for each sample at this point in the graphs was found to be 0.00318m.

Two trials were done for both samples. Finally, the hardness of each sample was calculated using the equation

$$HB = \frac{2P}{pD(D - \sqrt{D^2 - d^2})} \quad \text{Eq. 5}$$

where HB is the Brinell hardness number and P is the load corresponding to the diameter of the hole, d.

BEST VALUE CALCULATIONS

The best value of a mechanical property for one set of polyethylene samples was taken to be the mean of the values of the mechanical property for the individual samples in the set. For instance, to find the best value of the heat of fusion for the argon gamma radiated samples, the average of the heat of fusion values for the individual argon gamma radiated samples was calculated and taken to be the best value. To find the percent error of the best value, the standard deviation of the values of the mechanical property for the individual polyethylene samples was taken. Based on this standard deviation, the 95% confidence error of the values of the mechanical property for the individual polyethylene was found. The quotient of the 95% confidence error and the best value gives the percent

error of the best value. The sum of the best value and the 95% confidence error and the difference between these two values form the ends of the 95% confidence interval of the best value of the mechanical property for the set of samples. Theoretically if an additional value for the mechanical property is taken, there is a 95% chance that that value would fall within the range of mechanical property values covered in the 95% confidence interval.

RESULTS

Test	Argon	Air
<u>Day 1</u> Percent Crystallinity (95% Confidence Interval)	82.6 ± 1.02% (83.4 – 81.8)	80.7 ± 1.81% (82.2 – 79.2)
<u>Day 15</u> Percent Crystallinity (95% Confidence Interval)	82.1 ± 1.35% (83.2 – 81.0)	80.2 ± 1.82% (81.6 – 78.7)
Heat of Fusion (J/g) (95% Confidence Interval)	128 ± 2.03% (131 – 125)	132 ± 3.05% (136 – 128)
Young's Modulus (GPa) (95% Confidence Interval)	1.19 ± 12.4% (1.34 – 1.04)	2.03 ± 0.841% (2.04 – 2.01)
Yield Strength (MPa) (95% Confidence Interval)	45.2 ± 14.4% (51.7 – 38.7)	69.8 ± 12.6% (78.6 – 61.0)
Brinell Hardness Number (MPa) (95% Confidence Interval)	48.4 ± 2.27% (49.5 – 47.3)	49.7 ± 3.38% (51.4 – 48.1)

Table 1: The values of the mechanical properties for the UHMWPE samples.

The “Argon” column represents the samples that underwent gamma radiation treatment in the presence of argon gas and the “Air” column represents the samples that underwent gamma radiation treatment in the presence of air. Each number represents the best value of the mechanical property. The percent error is calculated from the best value of the mechanical property and is dictated by the 95% confidence interval for the best value.

The 95% confidence intervals for the percent crystallinity of the argon gamma radiated samples taken at Day 1 of the experiment overlap with those of the argon gamma radiated samples taken at Day 15. The same holds true for the air gamma radiated samples. Additionally, for each of these days the 95% confidence intervals for the percent crystallinity for the argon and air gamma radiated samples overlap.

The 95% confidence intervals for the heat of fusion and the Brinell hardness number values of the argon gamma radiated samples overlap with the corresponding values of the air gamma radiated samples. However, the 95% confidence intervals for the Young's modulus and the yield strength values of the argon gamma radiated samples do not overlap with the corresponding values of the air gamma radiated samples. These two values of these two mechanical properties, which indicate the “bending” strength of the polyethylene samples, were higher for the air gamma radiated samples than for the argon gamma radiated samples.

The heat of fusion and percent crystallinity values only concern the surface of the original “uncut” polyethylene samples because pieces were cut from the surface of the original samples and were tested.

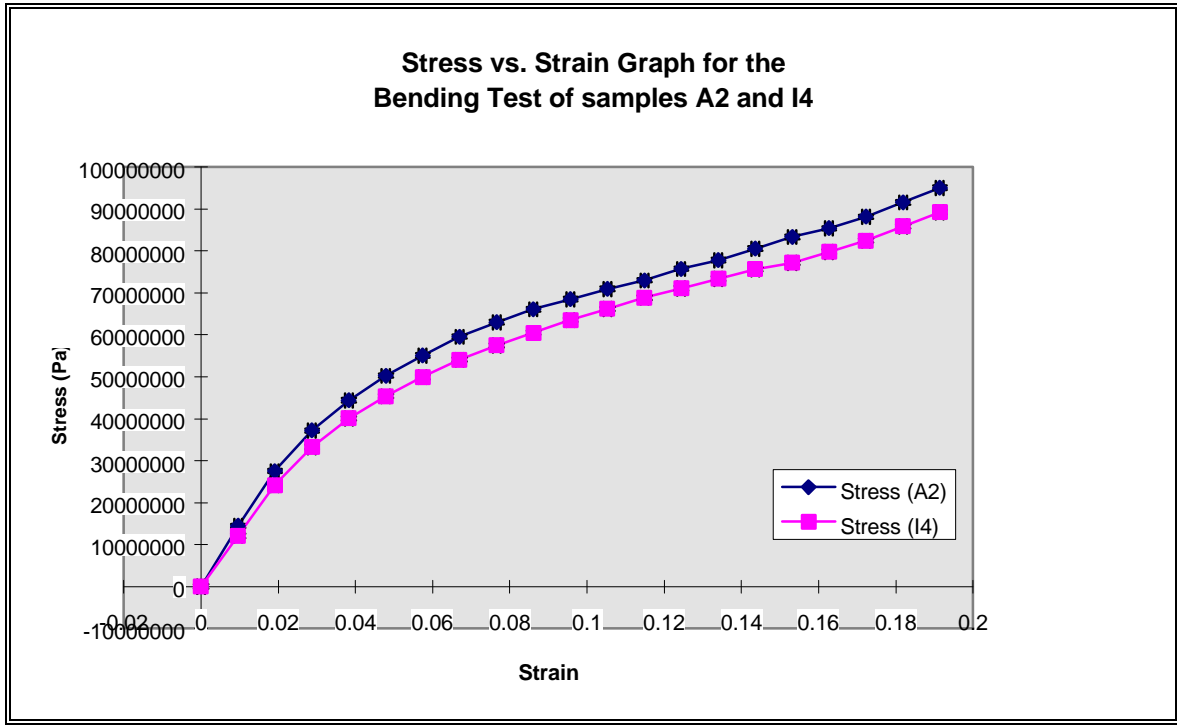


Figure 6: Independent Stress-Strain Graphs.

A2 is the sample gamma radiated in air and I4 is the sample gamma radiated in the presence of argon. The slope of linear (beginning) portion of the air sample is greater than that of the argon sample, signifying a greater Young’s modulus for the air sample. Also for similar stress values, the air sample experiences less strain than the argon sample does, indicating that the air sample has a greater “bending” strength. Also the curves are statistically distinct from each other because for the majority of each curve, the error bars of the curves do not overlap. However, nothing about the relative yield strength and toughness of the two samples is indicated by the graphs.

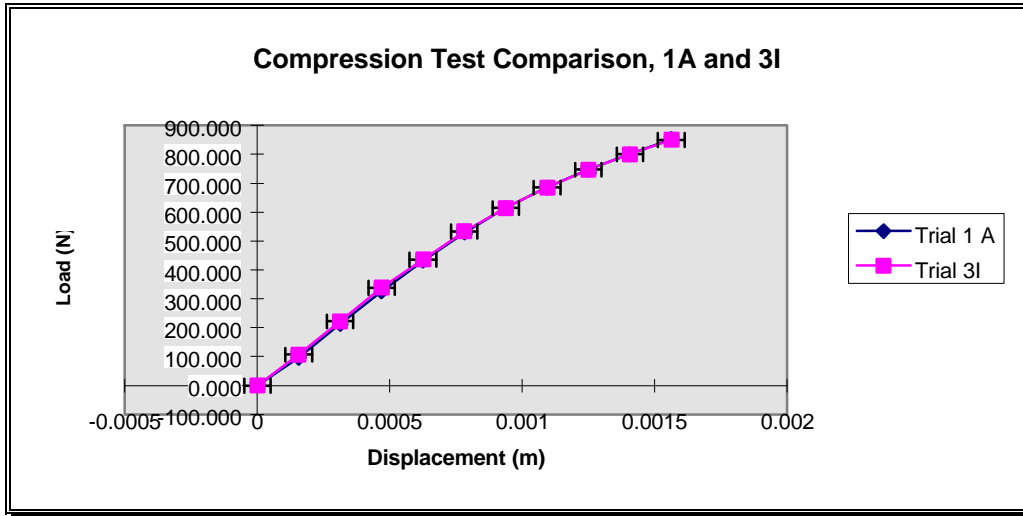


Figure 7: Overlapping Load vs. Displacement Graph of Compression Test.

A1 is the air sample and 3I is the argon sample. The error bars for the two graphs overlap, indicating that the two curves are statistically similar. The fact that the curves overlap for much of the region indicates their similarity. This signifies that the "compression" strengths of the two samples are statistically the same.

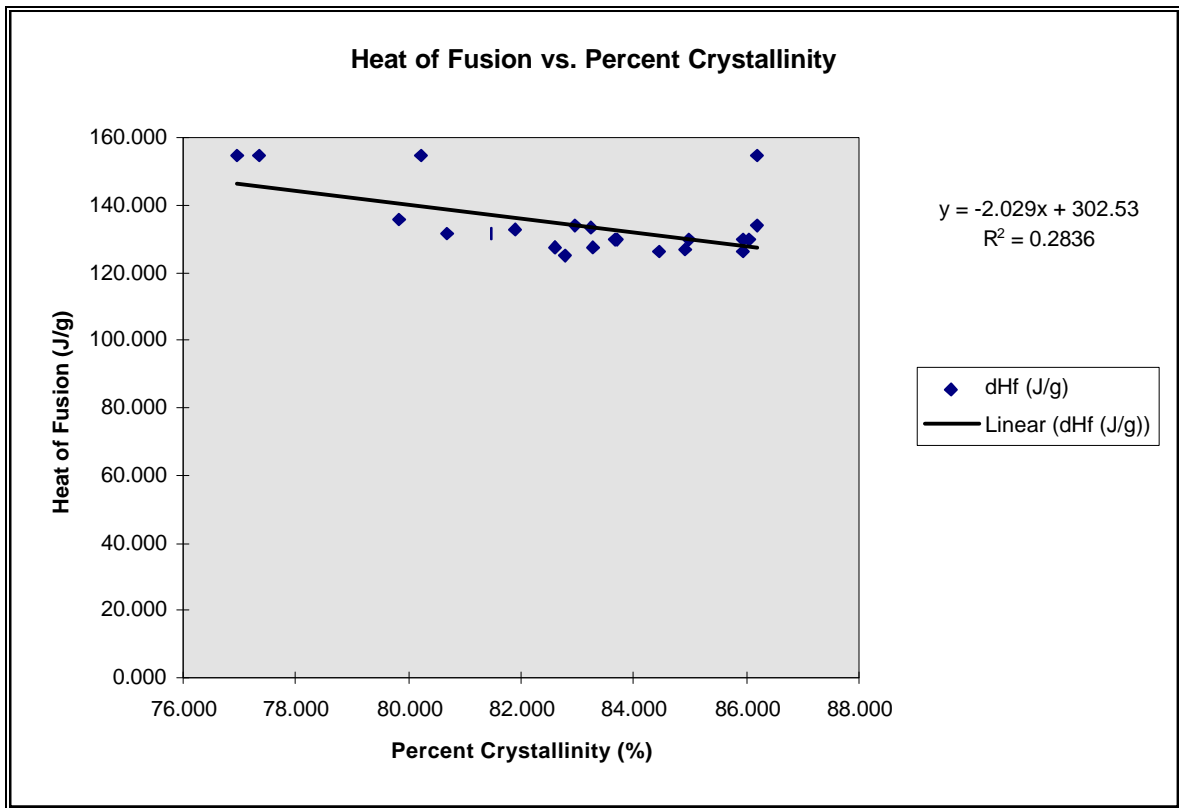


Figure 8: Relationship between percent crystallinity and heat of fusion.

The heat of fusion is related to the percent crystallinity as shown in figure. The graph was constructed from data provided by the DSC. For the full data arrays, please see APPENDIX B: DATA.

ERROR ANALYSIS

The effect of some sources of experimental errors on the results were quantified. These sources of errors contributed to the percent errors of the best values of the mechanical properties for the argon and air polyethylene samples. The maximum possible contribution of the quantified source to the percent error (95% confidence) of the best values of the pertinent mechanical properties for a set of samples was found. If, hypothetically, all other sources of experimental errors were eliminated then the maximum possible contribution of the quantified source of error would be the maximum possible percent error in the best value of the mechanical property of the set of samples. From comparisons between maximum possible contribution of the quantified source with the actual percent error of the best value, speculations about the actual contribution of the quantified source of error to the percent error of the best values were made. These speculations about the quantified sources of errors is covered in the “quantitative” error assessment portion of discussion.

During the DSC portion of the experiment, there was inaccuracy in measuring the masses of the papers that corresponded to the “amorphous” and “crystalline” regions of the heating curves. To find the error in the best value of the percent crystallinity resulting from this source of error, the formula:

$$dX = \frac{d(m_c)}{(m_c + m_a)} - \frac{m_c}{(m_c + m_a)^2} d(m_c + m_a) \quad \text{Eq. 6}$$

was derived and used, where $d(X)$ is the error of the crystallinity, and m_c and m_a are errors in the measurements of the masses of the crystalline and amorphous portions of the heating curve papers. Dividing $d(X)$ by the percent crystallinity of the samples gives the contribution of the source of error to the percent error of the percent crystallinity.

Concerning the heat of fusion results, the percent error contribution from the inaccuracy in measuring the mass of the samples was found to be the percent error of the mass reading. For the quantitative error assessments of both the percent crystallinity and heat of fusion results, masses of the heating curve papers and the polyethylene samples were taken from a representative polyethylene sample (Argon sample #1).

For the Young’s modulus results, the maximum percent error contribution to the best value by the inaccuracy of the measurements of the geometric properties of the polyethylene and the inaccurate readings from the force vs. displacement graphs, was found. From eqs.1 and 2, the differential method was used to derive the formulas:

$$d\mathbf{s} = \frac{LdP}{\left(\frac{8}{12} \cdot wx^2\right)} + \frac{PdL}{\left(\frac{8}{12} \cdot wx^2\right)} + \left[\frac{PL}{\left(\frac{8}{12} \cdot w^2x^2\right)} \right] dw - \left[\frac{2PL}{\left(\frac{8}{12} \cdot wx^3\right)} \right] dx \quad \text{Eq. 7}$$

$$d\mathbf{e} = \frac{12x}{L^2} d\mathbf{g} - \frac{24x\mathbf{g}}{L^3} dL + \frac{12\mathbf{g}}{L^2} dx \quad \text{Eq. 8}$$

where $d\sigma$ and $d\epsilon$ are errors in the stress and strains, respectively. Using these errors the error in the Young's modulus was calculated using the formula:

$$dE = \frac{d\mathbf{s}}{\mathbf{e}} - \frac{\mathbf{s}}{\mathbf{e}^2} d\mathbf{e} \quad \text{Eq. 9}$$

where dE is the error in the Young's modulus. The geometric measurements and force vs. displacement and stress vs. strain graphs for one representative polyethylene sample (Argon #3) was used for these quantitative error assessment calculations. The maximum contribution from any deviation from linearity of the linear portion of the stress vs. strain graphs, was found as the standard error of the slope of the best fit line through the linear portion of the stress vs. strain graphs. Linear regression was used to give the standard error of the slope.

For the yield strength results, maximum percent error contribution to the best value by the inaccuracy of the measurements of the geometric properties of the polyethylene and the inaccurate readings from the force vs. displacement graphs was equated with that found for the Young's modulus. Hence, Argon #1 was the representative polyethylene sample used here, also. The percent error contribution of this source of error for the yield strength was equated with that for the Young's Modulus, because the same stress vs. strain graphs were used for the calculation of the yield point for each sample as that of the Young's modulus. The maximum error contribution arising from the inaccuracy of the ".2% offset" line was also quantified. From the ".2% offset" line, differential method was used to derive the formula:

$$d\mathbf{s} = (\mathbf{e} - 0.002)dE + Ede \quad \text{Eq. 10}$$

$d\sigma$ divided by the yield point gives the maximum contribution of error by the inaccuracy of the ".2% offset" line to the percent error of the yield point. Again the geometric property measurements, force vs. displacement and stress vs. strain graphs, and ".2% offset" line for one polyethylene sample (Argon #3) was used for these quantitative error assessments.

The maximum error contribution to the best values of Brinell hardness numbers by the inaccurate measurements of the diameter of the ball and the readings from the force vs. displacement graphs was found. Using the differential method, Eq.4 was partially derived to yield the formulas:

$$d(HB) = \frac{2dP}{y} - \frac{2Pdy}{y^2} \quad \text{Eq. 11}$$

$$dg = 2pDdD - pxdD - pDdx \quad \text{Eq. 12}$$

$$dx = \frac{D \cdot dD}{\sqrt{D^2 - d^2}} - \frac{d \cdot d(d)}{\sqrt{D^2 - d^2}} \quad \text{Eq. 13}$$

Here the error in the readings for the diameter of the hole in the polyethylene (resulting from the compression load of the ball) was equated with the error reading of the displacement value of 0.000675m, from the force vs. displacement graphs. Argon #3 was the choice for the representative polyethylene sample for this quantitative error assessment.

	Maximum contribution to the percent error of the best value (actual percent error of the best value in bold corresponding to the mechanical property for argon, air)
Percent Crystallinity	(1.02% , 1.81%) (1.35% , 1.82%)
Inaccurate Mass Readings (Paper)	2.56%
Heat of Fusion	2.03% 3.052%
Inaccurate Mass Readings (Polyethylene samples)	7.92%
Young's modulus	12.4% .841%
Inaccurate measurements of the geometric properties of the Polyethylene samples and reading from the force vs. Displacement graphs	5.25%
Non-linearity of the elastic portion of the stress vs. Strain graphs	6.51%
Combination of the two sources of errors	11.76%
Yield Point	14.4% 12.6%

Inaccurate measurements of the geometric properties of the Polyethylene samples and reading from the force vs. Displacement graphs	5.25%
Inaccurate "0.2% offset line"	2.88%
Combination of the two sources of errors	8.13%
Brinell Hardness number	2.27% 3.38%
Inaccurate measurement of the diameter of the ball and reading from the force vs. Displacement graphs	2.48%

Table 2 Summary Table of Error Analysis.

The sources of error can contribute as much as their listed percentages to the percent error of the best values of the properties under which the sources of error are listed. For the percent error of the best value of the listed properties, the first percentage corresponds to the argon samples and the second corresponds to the air samples. However for the percent error for the best value of the percent crystallinities, the first parenthesis corresponds to samples taken at Day 1 of the experiment and the second parenthesis corresponds to the samples taken at Day 15. In each parenthesis, the first percentage corresponds to the argon samples and the second, to the air samples.

DISCUSSION

SIGNIFICANT FINDINGS

The results show that the best value (mean) of the percent crystallinity of the argon gamma radiated samples taken at the beginning of the experiment (Day 1) was statistically the same as that of the argon gamma radiated samples taken later in the course of the experiment (Day 15). This can be concluded on the basis that the 95% confidence intervals of these two values overlap, indicating that the reason why the best values are not exactly the same is because of experimental error or chance. The quantitative assessment of particular sources of errors on our results is covered later in the discussion (please see the QUANTITATIVE ERROR ASSESSMENT section). The 95% confidence intervals of the best value of the percent crystallinity of the air radiated samples taken at Day 1 also overlaps with that of the air radiated sample taken at Day 15, meaning that the two values for the percent crystallinity were also statistically the same. These results show that during the course of this part of the experiment, the percent crystallinities of the two sets of samples did not change significantly.

The 95% confidence intervals for the best values of the percent crystallinity of argon and air radiated samples, taken at Day 1, overlap. And the same holds true for the samples taken at day 15. These two findings indicate from Day 1 to Day 15 of the experiment, the percent crystallinities of the two sets of samples were statistically the same.

The 95% confidence intervals of the best value of the heat of fusion for the argon and air radiated samples overlap. The same holds true for the 95% confidence intervals of the best values of the Brinell Hardness numbers for both sets of samples. These results demonstrate that the heat of fusion and the hardness for the two sets of samples were statistically the same.

However, the 95% confidence intervals for the best values of both the Young's moduli and the yield strengths of the two set of samples do not overlap, indicating that both of these properties for one set of samples were statistically different from the corresponding values of the other set. Also, the best values for the Young's modulus and the yield strength of the argon radiated samples were actually lower than those of the air radiated samples. These results indicate that the "bending" strength of the air radiated samples is greater than that of the argon radiated samples.

QUANTITATIVE ERROR ASSESSMENT

The maximum possible contribution to the 95% confidence interval of the best values of the percent crystallinity from the imprecision in the taking of the masses of the crystalline and amorphous regions of the melting curves of both sets of samples is 2.56%. The percent errors of the best values of the percent crystallinities of both sets of samples

taken at Day 1 (argon: 1.02%, air: 1.81%) and Day 15 (argon: 1.35%, air: 1.82%) are under this maximum value from this source of error. Therefore, it is possible for this source of error to be responsible for majority of the range of the 95% confidence interval.

The inaccuracy with which the software associated with the DSC displays the “amorphous” and “crystalline” regions of the heating curve is another source of error. Here the software does more than just take and display measurements. It bases its division of the melting curve between the “amorphous” and “crystalline” regions on calculations done on the curve. Additionally, the data and calculations of the DSC could be skewed by irregular placement of the “base” line of the melting curve. Error associated with these calculations also contributes to the 95% confidence interval. However, due to the nature of the software, the possible error is unquantifiable.

The imprecision in taking the mass of the polyethylene samples can account for as much as 7.92% error in the best value for the heat of fusion of the two samples. However, the percent errors for best values for both samples (argon: 2.03%, air: 3.05%) are less than 7.92% meaning that this source of error could have accounted for majority of the 95% confidence interval. Nonetheless, the imprecision with which the software calculates the heat gone into melting the samples may be another substantial source of error.

Errors in the measurements of the dimensions (length, width, height, and notch depth) of the samples and reading from the force vs. displacements graphs is another source of error. These measurements and readings were used to translate the force vs. displacement graphs to stress vs. strain graphs for each sample. This source of error could have contributed as much as 5.25% error in the best value of the Young’s modulus. Another source of the error results from the deviation from linearity of the “elastic deformation” portion of the stress vs. strain graphs. This source of error could have contributed as much as 6.51% error in the Young’s modulus value. The combination of the maximum contributions of errors (11.78%) from the two aforementioned sources of errors is greater than the actual percent error of the Young’s modulus for the air samples (.841%) but is less than that for the argon samples (12.4%). The two sources of error may not account for the majority of the percent error of the best values of the Young’s modulus for the argon samples but most likely accounts for the majority of the percent error for the air samples.

Inaccuracies in the measurements of the dimensions of the samples also could have contributed as much as 5.25% error to the best values of the yield strengths of the two sets of samples. The imprecision of the “2% offset” equation, used in the yield strength calculations, $y = E(x - 0.002)$ could have contributed as much as 2.88% error. The combination of these two maximum possible sources of error (8.13%) is less than the actual percent errors (argon: 14.4%, air: 12.6%) of the best values for the yield strengths of the two sets of samples. Again, these two sources of errors can contribute to most of the percent errors in the best values.

The imprecision in the measurements of the diameter of the ball and reading the load and displacement from the load vs. displacement graphs can contribute as much as 2.48% error in the best value of the Brinell hardness numbers for the two set of samples. This maximum contribution is less than the percent errors of the best value for the air samples but greater than that for the argon samples, indicating that this source of error may have not accounted for the majority of the percent errors of the best values for the air samples but most likely accounts for the majority of the percent errors for the argon samples.

LIMITATIONS OF THE FINDINGS AND POSSIBLE EXPERIMENTAL ALTERATIONS

One source of error that we could not quantify in this experiment was the imprecision with which the software, associated with the differential scanning calorimeter setup, made its calculations to find the heat of fusion of the samples and allot “crystalline” and “amorphous” portions to the melting curve. One way to quantitatively assess this source of error is to run test samples of known percent crystallinity and heat of fusion through the DSC setup. Comparing expected heating curves and the results for the heat of fusion with the actual ones provided by the software would enable quantitative assessment of the maximum contribution of percent error by the software to the best values of the heat of fusion and percent crystallinity. Here, any discrepancies between the expected heating curves and heat of fusion results and the actual ones would provide an assessment of the error from the software.

Since oxidation is a function of time, the analysis of the experiment is significantly hindered by the fact that two important conditions were not provided: 1) the sterilization dates of the two samples and 2) the initial percent crystallinities of the samples. Without these two pieces of information, cross-analysis of the air- and argon-sterilized samples are inconclusive. For the purposes of this analysis, it has been assumed that the two samples were sterilized at approximately the same time (within a period of days) and that they had similar (but not necessarily identical) percent crystallinities.

Another limitation of this experiment was that we did not know and were not able to determine whether the polyethylene samples had reached their maximum oxidation capacity. The samples will become oxidized until a plateau is reached where the samples can not undergo any more substantial oxidation and, hence, the samples are at their maximum crystallinity. At this point, the maximum effect from the radiation treatment on the samples is achieved. There is a good possibility that the polyethylene samples did not reach their maximum oxidation capacities. If there was room for considerable oxidation of the samples, then the mechanical properties of the samples could have the same potential to change over time because they are contingent upon the percent crystallinity of the samples (Naidu et al., 1996). In this case, comparisons between the mechanical properties of the two sets of sample may be more inconclusive because these results would change if this experiment had been conducted with the same samples at a later date. Although the results show that the sample did not undergo measurable oxidation during the 15 day part of the experiment, they can not be used to conclude the oxidation capacity of the sample at a date much longer than

15 days after the experiment (e.g. one year from now). Due to time constraints, we were unable to verify the literature reports relating increased oxidation over time.

Another limitation concerning uncertainty of the state of the polyethylene samples, is that we did not know the percent crystallinities the argon and air samples immediately before and after their respective gamma radiation treatments. As discussed, this lack of information detracts the significance of our percent crystallinity results. Knowing these aspects of the previous states of the polyethylene samples would allow us to determine the increase in crystallinity. Also, un-irradiated polyethylene samples could have been incorporated in the experiments, where the percent crystallinity change of the samples from the two types of radiation could be measured, as well as a change in exposure to air a long time period post-radiation. Ideally, the sterilization of all of the polyethylene samples would occur on the same day, thus allowing all samples to have equal opportunity for oxidation. With this alteration, results for the percent crystallinities for the two sets of samples could justifiably be compared to quantify the effect of air exposure on the two sets of radiated samples.

To ensure that the two set of samples have reached their maximum oxidative capacities (hence, their maximum crystallinity), the polyethylene sample should be treated in a pressurized air chamber. The limiting reagent for the oxidation of the polyethylene samples is the diffusion of oxygen into the samples (Naidu et al., 1996). According to Fick's First Law of steady-state diffusion from Callister, p. 94,

$$J = -D \frac{dC}{dx}$$

Eq. 14

(where J is the diffusion flux, and D is the diffusion coefficient) if the polyethylene samples were treated in a pressurized chamber, oxygen would diffuse through the samples more quickly because the concentration gradient of oxygen between the outside and inside of the polyethylene would be greater (Callister, 1997). With the increase in the diffusion rate of oxygen, the polyethylene would reach closer to their maximum oxidation state and the attainment of near maximum percent crystallinity of the polyethylene samples would be insured. This would substantiate any comparisons of the mechanical properties between the two sets of samples because the mechanical properties would not substantially change significantly over time.

Another limitation of this experiment is that we were unable to quantitatively compare the effects of argon and air gamma radiation on the polyethylene samples *in vivo*. The two types of treatments may differ in the way they change the oxidative capabilities of the polyethylene samples in the human body. For instance, the treatments may differ in the way they change the fluid absorptive properties of the polyethylene. The extent of biological fluid penetration may determine the magnitude of oxidation of the implanted polyethylene by various substances in the fluid by controlling the accessibility of potential oxidizing agents in the fluid with the interior of the implant (Naidu et al., 1996).

One experimental alteration that would make the experiment more significant, with this respect, is to treat the polyethylene samples in a simulated biological environment where the samples are exposed to a biological fluid. In many previous experiments, the samples were treated with cow serum at body temperature for several months before their mechanical properties would be measured (Naidu et al., 1996).

THEORETICAL EXPLANATION OF THE RESULTS

Theoretically, after the radiation treatment, the percent crystallinity of the air gamma radiated sample should be greater than that of the argon gamma radiated sample, assuming that the two samples had the same initial percent crystallinity. It is not necessarily the case that the two samples had the same percent crystallinity. For instance, allow the argon sterilized sample to have 30% crystallinity and the air sterilized sample to have 10% crystallinity pre-sterilization. After gamma irradiation, the argon sample will remain at 30% crystallinity, but the air sample will increase in crystallinity, perhaps to an equal amount as the argon sample (30%). In this case, if the samples are tested immediately after sterilization, they will have the same crystallinity. This is one scenario that justifies the results from this experiment.

In another scenario, the two samples have the same initial crystallinity (arbitrarily, 30%) before sterilization. After gamma sterilization, the air irradiated sample will have greater crystallinity (50%) than the argon (30%). However, if the exposure to oxygen after sterilization is long enough, oxidation of the argon sample will occur such that the percent crystallinity of the argon sample will become similar to that of the air sample because argon has greater capacity to undergo oxidation after the radiation sterilization. This possibility can explain the matching percent crystallinities of the two sets of samples (Naidu et al., 1996). In this case, the argon sample may have been made significantly earlier and allowed to age for a longer period of time than the air sample. Thus, at sterilization the argon sample may have a greater crystallinity (50%) than the air sample (30%), and after sterilization, their crystallinities may be the same (50%). This scenario also provides an explanation for the similar percent crystallinities in our experiment.

Therefore, it is possible that one of the set of samples may have been tested in this experiment a short time after its sterilization treatment, and the other may have been tested a long time after its treatment. In short, the percent crystallinities of the two sets of sample before and after their sterilization treatments and the date of their treatments are required in order to determine which of the above scenarios would explain the results from the experiment.

The results for the percent crystallinities of the two sets of samples explain the results for their heat of fusion values. The heat of fusion values of UHMWPE samples are contingent upon the differences of the percent crystallinities of the samples (BE 210 Lab Manual, 1997). Since the results show that the percent crystallinities of the two sets of samples are the same, the results should also show a similarity in the two heat of fusion

values, which they do. Also the pertinence of the percent crystallinity and heat of fusion results is limited to the surface of the “original” (uncut) polyethylene samples because samples for the DSC were cut from the surface.

However, the results for the percent crystallinities of the polyethylene samples can not explain the fact that our results for the Young’s moduli and the yield point of the samples. Explanation for these results may be based on the way the polyethylene samples, to be tested with the Instron, were cut from the original sample.

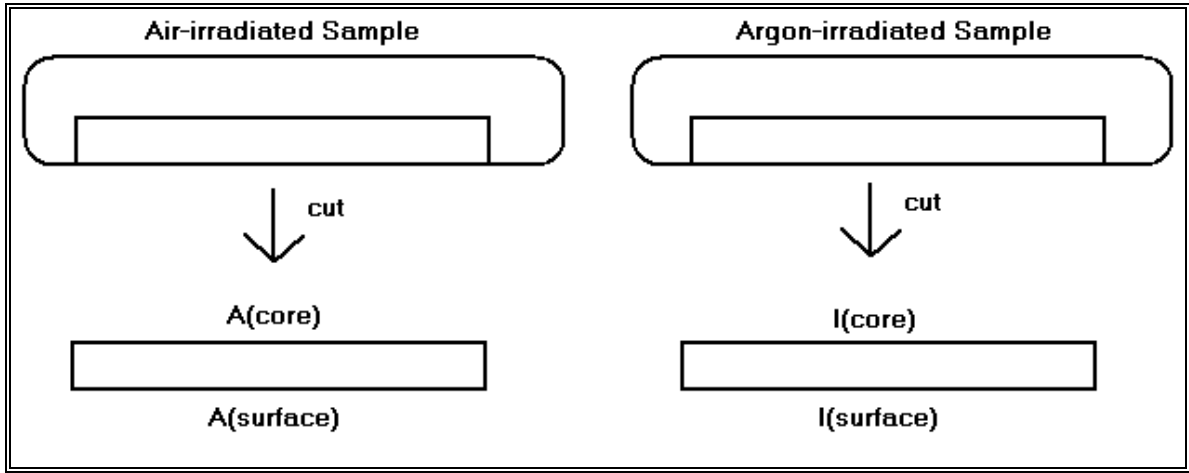


Figure 9: Schematic representation of the tested samples cut from the original implants.

It is probable that the interior core of the polyethylene samples were less oxidized than the surface of the original samples. It follows that the core of the sample is less crystalline and will have better “bending” properties (higher Young’s modulus and yield strength). The cores of the samples are more ductile than the surface because they are less crystalline. After the samples are cut from the original, the two sides were indistinguishable from one another. Thus, if the argon irradiated sample was tested with its surface side in tension during the three point bending test, I(surface), and the air irradiated sample was tested with its core side in tension, A(core), then the air sample would demonstrate greater “bending” properties, as shown by the results.

A less probable explanation of the Young’s modulus and yield point results is that the inner core of the argon radiated original sample is more oxidized than that of the air radiated original sample probably because the more oxygen had diffused to the inner core of the argon original sample. In this case, if sides of the two sets of samples, that were formerly the inner core of their original sample, were in tension, our results would be obtained. This is so because the sides of the air sample that were held in tension would be stronger than those of the argon sample, due to a lesser degree of oxidization of these sides of the air samples.

However, for the hardness tests, the sides of the two sets of cut samples that were subject to compression under the ball could have had the same crystallinity, meaning that all of the hardness tests were performed on either the core or surface of both samples. It is most probable that both samples were tested on their surface sides, I(surface) and A(surface), since they had the same crystallinity. The similar crystallinity would yield similar hardness numbers, as is consistent with the data.

However, sometimes another carbon chain replaces one of the hydrogen atoms of the ethylene molecule (some other alkane or alkene is polymerized). In this case, the polymer becomes branched. Linear and branched polyethylene can be represented as follows:

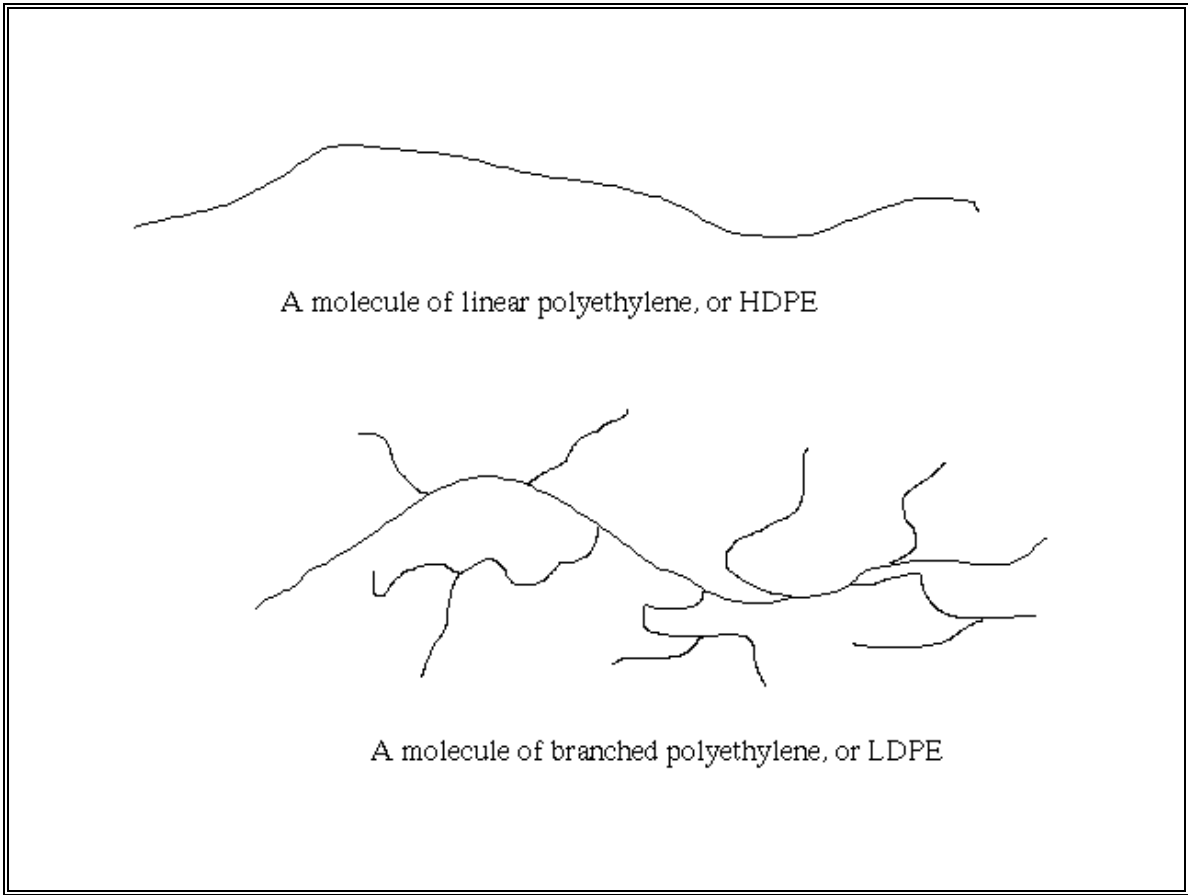


Figure 11: Schematic Diagram of Linear vs. Branched Polyethylene

Linear PE forms a polymeric fiber, a polymer whose chains are stretched out straight (or close to straight) and lined up next to each other, all along the same axis, similar to the diagram below:

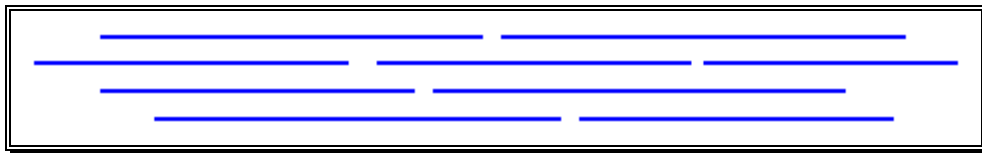


Figure 12: Schematic representation of a polymeric fiber.

Polymeric fibers are significantly stronger than bulk materials (Callister, 1997) and have been used to replace Kevlar in bulletproof vests (University of Southern Mississippi, Department of Polymer Science, 1996).

APPENDIX B: DATA

COMPRESSION TESTS

	Trial 1 A	Trial 2 A	Trial 3 I	Trial 4 I	Trial 6 A
Disp (in)	Load (lb)	Load (lb)	Load (lb)	Load (lb)	Load (lb)
0.000	0.000	0.000	0.000	0.000	0.000
0.006	21.500	21.000	24.000	24.000	24.000
0.013	48.000	51.000	50.000	50.000	52.000
0.019	73.000	78.000	76.000	74.000	79.000
0.025	97.000	103.000	98.000	98.000	105.000
0.031	119.000	126.000	120.000	118.000	127.000
0.038	138.000	145.000	138.000	137.000	146.000
0.044	154.000	162.000	154.000	153.500	163.000
0.050	168.000	175.500	168.000	167.000	176.000
0.056	180.000	186.500	180.000	179.000	188.000
0.063	191.500	196.000	191.000	190.000	198.000

Table 3: Compression Data for Hardness Tests.

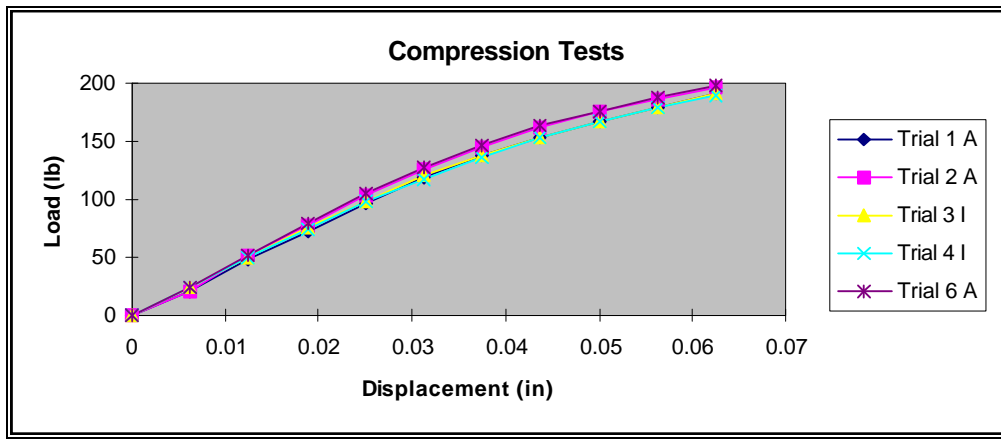


Figure 14: Graphs of the Compression Data.

THREE-POINT BENDING

Displacement (in)	Trial 1 - A Load (lb)	Trial 2 - A Load (lb)	Trial 3 - I Load (lb)	Trial 4 - I Load (lb)
0	0	0	0	0
0.005	11	10.5	10	8
0.01	19.5	20	18.5	16

0.015	26.75	27	24.5	22
0.02	33	32.25	29.75	26.5
0.025	38.25	36.5	34	30
0.03	42	40	37.5	33
0.035	44.5	43.25	40.75	35.75
0.04	46.75	45.75	43.5	38
0.045	48.5	48	46	40
0.05	49.75	49.75	48.5	42
0.055	51	51.5	50	43.75
0.06	52.5	53	52	45.5
0.065	54	55	53.5	47
0.07	55.5	56.5	55	48.5
0.075	57	58.5	56.5	50
0.08	58.5	60.5	58	51
0.085	60	62	59.5	52.75
0.09	62.5	64	61.5	54.5
0.095	65	66.5	63.5	56.75
0.1	68.5	69	65.75	59

Table 4: Three-Point Bending Data

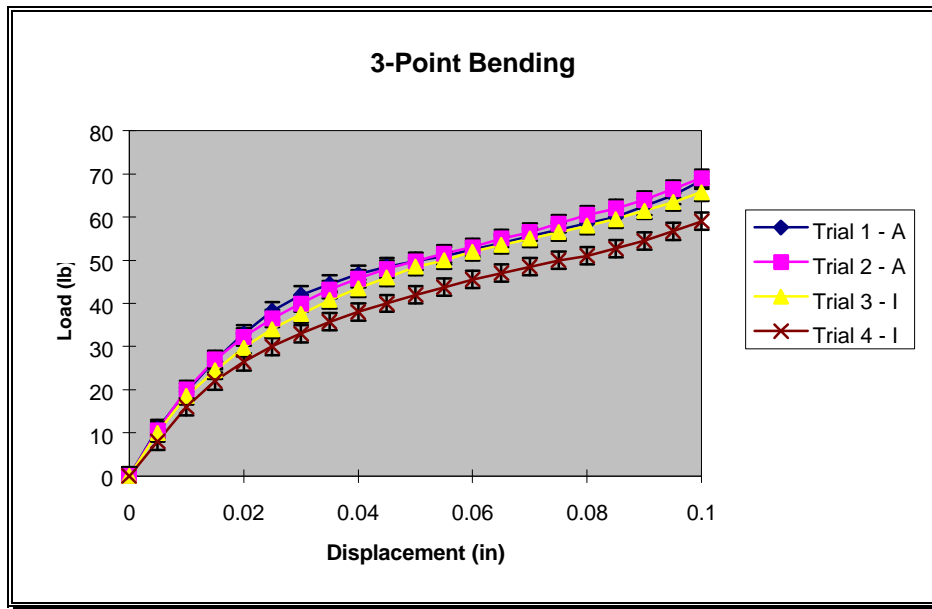


Figure 15: Three-Point Bending Graphs

DIFFERENTIAL SCANNING CALORIMETRY

Sample	Sample (mg)	Area (mJ)	dHf (J/g)	Curve Mass (mg)	Cryst. Mass (mg)	Percent Crystallinity
Indium 1	15.509	435.822	28.101	101.080	10.080	100.000
Indium 2	14.138	411.522	29.107	27.000	10.080	100.000
Average	14.824	423.672	28.604	64.040	10.080	100.000
Std. Dev	0.969	17.183	0.711	52.382	0.000	0.000
	Sample (mg)	Area (mJ)	dHf (J/g)	Curve Mass (mg)	Cryst. Mass (mg)	Percent Crystallinity
Argon 1	12.620	1,656.541	131.263	301.900	24.590	81.451
Argon 2	7.322	962.097	131.398	170.500	13.760	80.704
Argon 3	13.519	1,754.836	129.805	313.500	26.230	83.668
Argon 4	8.021	1,022.191	127.439	181.900	15.150	83.288
Argon 5	6.873	858.730	124.943	152.300	12.610	82.797
Argon 6	6.676	866.472	129.789	160.000	13.390	83.688
Argon 7	6.847	872.096	127.369	153.400	12.670	82.595
Average	8.840	1,141.852	128.858	204.786	16.914	82.599
Std. Dev	2.935	390.735	2.365	71.122	5.884	1.137
Argon 8	4.647	619.561	113.325	93.000	79.000	84.946
Argon 9	8.781	1,176.391	133.970	181.000	156.000	86.188
Argon 10	6.299	835.863	132.698	127.000	104.000	81.890
Argon 11	6.563	829.984	126.464	121.000	104.000	85.950
Argon 12	8.862	1,225.782	126.998	192.000	163.000	84.896
Argon 13	9.449	1,415.729	126.439	206.000	174.000	84.466
Argon 14	7.204	977.008	129.500	165.000	142.000	86.061
Average	7.401	1,011.474	127.056	155.000	131.714	84.914
Std. Dev.	1.721	275.412	6.769	41.893	36.003	1.492
Total Av.	8.120	1,076.663	127.957	179.893	74.314	83.756
	Sample (mg)	Area (mJ)	dHf (J/g)	Curve Mass (mg)	Cryst. Mass (mg)	Percent Crystallinity
Oxygen 1	9.560	1,316.024	137.659	134.200	10.630	79.210
Oxygen 2	8.121	1,142.214	140.649	208.900	16.820	80.517
Oxygen 3	8.805	1,174.574	133.399	206.500	17.190	83.245
Oxygen 4	8.519	1,155.347	135.620	210.300	16.790	79.838
Average	8.751	1,197.040	136.832	189.975	15.358	80.703
Std. Dev.	0.608	80.428	3.083	37.216	3.157	1.777
Oxygen 5	11.510	1,782.101	154.831	268.000	215.000	80.224
Oxygen 6	8.836	1,335.116	151.100	203.000	175.000	86.207

Oxygen 7	6.554	1,014.270	154.756	150.000	116.000	77.333
Oxygen 8	8.014	1,192.199	148.765	178.000	137.000	76.966
Average	8.729	1,330.922	152.363	199.750	160.750	80.183
Std. Dev.	2.081	328.173	2.964	50.388	43.638	4.272
Total Av.	8.740	1,263.981	144.597	194.863	88.054	80.443

Table 5: Heat of Fusion and Percent Crystallinity Data from the DSC.

REFERENCES

1. Alberts, Bruce, et al. Molecular Biology of the Cell, Third Edition. Garland Publishing, Inc. New York, NY. 1994.
2. Association for the Advancement of Medical Instrumentation. AAMI Recommended Practice: "Process Control Guidelines for Gamma Radiation Sterilization of Medical Devices." ISBM-0-910275-38-6. pp. 7-21. 1984.
3. Association for the Advancement of Medical Instrumentation. AAMI Recommended Practice: "American National Standard Guideline for Gamma Radiation Sterilization." 1991.
4. American Association of Orthopedic Surgeons. *Gamma Sterilization Increases Oxidation, Says Study* (<http://www.aaos.org/wordhtml/aaosnews/gamma.htm>). February 23, 1996.
5. Beer & Johnston. Mechanics of Materials. McGraw-Hill, Inc. New York, NY. 1992. Chapters 1, 2, and 4.
6. Berger, Lukas; Plummer, Christopher J. G.; and Kausch, Hans-Henning. Deformation and Structure in UHMWPE Fibers (<http://sdmac6.epfl.ch/LP/LP-page/LB/LBtext>).
7. Berkley Orthopedics Biomechanics. Homework #5. Department of Mechanical Engineering. University of California at Berkley. 1993 (<http://biomech2.berkeley.edu/me176hw/hw5.html>).
8. Bioengineering 223 Course Manual. University of Pennsylvania. Philadelphia, PA. Spring 1997.
9. Bioengineering Laboratory I Manual. *Experiment 9: Three Point Bending*. University of Pennsylvania. Philadelphia, PA. Fall 1996.
10. Bioengineering Laboratory II Manual. *Experiment 5: Material Science of the Artificial Hip*. University of Pennsylvania. Philadelphia, PA. Spring 1997.
11. Callister, William D. Jr. Materials Science and Engineering: An Introduction. Fourth edition. John Wiley and Sons, Inc. New York, NY. 1997.
12. Campbell, Neil A. Biology, Third Edition. The Benjamin/Cummings Publishing Company, Inc. Menlo Park, CA. 1993.
13. Candor Technologies (<http://www.candor.com/medical/knees.htm>). *Total Knee Replacement*. 1996.
14. Chang, Raymond. Chemistry, Fourth Edition. McGraw Hill, Inc. Hightstown, NJ. 1991.
15. Chang, Raymond. Physical Chemistry with Applications to Biological Systems, Fourth Edition. MacMillan Publishing Co., Inc. New York, NY. 1981.
16. Fox, Stuart Ira. Human Physiology, Fifth Edition. Wm. C. Brown Publishers. Chicago, IL. 1996.
17. Hochman, Mary, MD; Rundle, Debra, MSBE; University of Pennsylvania Health Systems; Visible Human Project; and National Library of Medicine. *Interactive Knee* (<http://www.rad.upenn.edu/rundle/InteractiveKnee.html>). 1995.
18. Hutchings, Ian. *Joint Project* (http://www.msm.cam.ac.uk/material_eyes/2/joint.html).
19. Isomedix. *Choosing Your Sterilization Process*, <http://www.isomedix.com/process.htm>.

20. Kocmond, Jonathon; Stern, Steve; Stulberg, David; Carter, Justin; and Piazza, Stephen. *Simulation-based Design of Total Knee Replacements* (<http://sulu.smpp.nwu.edu/~delp/proj2.html>). 1995.
21. de Langen, M.; Luigjes, H.; and Prins, K. O. *Phase Diagram of Polyethylene* (<http://gopher.phys.uva.nl:70/0/fnsis/onderzoek/nmr/nmrpeen.htm>).
22. Li, S.; Saum, K. A.; Collier, J. P.; and Kasprzak, D. *Oxidation of UHMWPE Over Long Time Periods*. Trans. Soc. for Biomaterials. pp. 425. 1994.
23. Lide, David, R. Handbook of Physics and Chemistry, 75th Edition. Special Student Edition. CRC Press. Ann Arbor, MI. 1994.
24. Naidu, Sanjiv H., MD; Bixler, Brian L., MD; and Moulton, Mark J. R., MD. "Radiation-Induced Physical Changes in UHMWPE Implant Components." *Orthopedics*. 1997; 20(2): 137-142.
25. *Orthopedics Research Lab* (http://ortholab.ahsc.arizona.edu/Ortho_Home_Page.html). University of Arizona, Department of Surgery. Arizona Health Sciences Center. Tucson, Arizona. 1995.
26. Ries, M.; Rose, R.; Greer, J.; Weaver, K.; and Beals, N. *Sterilization Induced Effects on UHMWPE Performance Properties*. Trans. ORS. pp. 757. 1995.
27. Riley, William F., Sturges, Leroy D., and Morris, Don H. Statics and Mechanics of Materials: An Integrated Approach. John Wiley & Sons, Inc. New York, NY. 1995.
28. Spanoudis, Steve & Koski, Greg. *sci.polymers FAQ* (<http://www.polymers.com/poly-faq.html>). 1995.
29. SteriGenics International (<http://www.sterigenics.com/medical/medical.htm>). *Medical Device Sterilization*.
30. Sun, D. C., PhD; Wang, A., PhD; Stark, C., MS; and Dumbelton, J. H., PhD *Development of Stabilized UHMWPE Implants with Improved Oxidation Resistance via Crosslinking*. Scientific Exhibition presented at the 63rd Annual Meeting of the American Academy of Orthopedic Surgeons (AAOS). Atlanta, GA, USA. February 22-26, 1996.
31. Sutula, L. C.; Collier, J. P.; Saum, K. A.; Currier, B. H.; Currier, J. H.; Sanford, W. M.; Mayor, M. B.; Wooding, R. E.; Sperling, D. K.; Williams, I. R.; et al. *Impact of gamma sterilization on clinical performance of polyethylene in the hip* (<http://www.medmedia.com/t4/68.htm>). Dartmouth Biomedical Engineering Center, Thayer School of Engineering. Clinical Orthopedics & Related Research. (319):28-40, 1995 Oct.
32. Tipler, Paul A. Physics for Scientists and Engineers, Third Edition. Volume 1. Worth Publishers, Inc. New York, NY. 1991. pp. 238-242.
33. University of Pennsylvania School of Veterinary Medicine (Dr. William J. Donawick, Jonathan Roth, and Molly Northrop). *Home Page for Surgical Principles Course #8001* (<http://phl.vet.upenn.edu/cal95/surgery/index.html>). 1996.
34. University of Southern Mississippi, Department of Polymer Science. *Polyethylene* (<http://www.psrc.usm.edu/macrog/pe.html>). 1996.
35. Wade, L. G., Jr. Organic Chemistry, Third Edition. Prentice Hall, Inc. Upper Saddle River, NJ. 1995.

36. Ward, Richard E., MD, MBA & and MacWilliam, Cynthia H., MBA. *Total Joint Replacement* (<http://www.hfhs-cce.org/document/tjrsum.htm>). Center for Clinical Effectiveness, Henry Ford Health System. Detroit, MI. 1995.
37. Williams, V. R. & Williams, H. B., 1973. Basic Physical Chemistry for the Life Sciences. Second Edition. San Francisco, WH Freeman & Co. Chapter 6.
38. Wright Medical Technology, Inc. (<http://ortho1.med.uth.tmc.edu/WMT/poly.htm>). *Effects of Sterilization Methods on Ultra-High Molecular-Weight Polyethylene (UHMWPE)*. Arlington, TN. 1995.
39. ZEUS, Inc. *Gamma Sterilization* (<http://www.zeusinc.com/technical/gamma.html>).
40. Zumdahl, Steven S. Chemistry, Third Edition. D. C. Heath and Co. Lexington, MA. 1993. p. 638.